

## Uniform Suction/ Blowing Effect on Micropolar Fluid Flow due to a Stretching Cylinder

**Dr.Mohammad Shafique**

507-70 Steenvale Drive, Toronto, Canada  
Ex-Assistant Professor of Mathematics,  
Gomal University, Dera Ismail Khan, Pakistan  
mshafique6161@yahoo.com

**Prof.M.Anwar Kamal**

Department of Mathematics,  
Al-Kharj University, Al-Kharj, Saudi Arabia

**Received: 13-06-2013**

**Revised: 23-07-2013**

**Accepted: 24-07-2013**

---

**Abstract:** *In this research work, the problem of uniform suction /blowing effect on flow and heat transfer due to a stretching cylinder is investigated numerically for micropolar fluids. The partial differential equations are converted in to ordinary differential equations by using similarity transformations. The resulting equations are solved by using successive over relaxation method and Simpson's (1/3) rule. The results have been obtained for various values of the parameters involved in the equations of motion, namely Reynolds number  $R$ , suction/ injection parameter  $\gamma$  and Prandtl number  $Pr$ , to study their effect on velocity and temperature fields as well as on the Nusselt number and the skin friction coefficient. The results are given both in tabular and graphical forms.*

AMS Subject Classification: 76M20.

**Key Words:** *Micropolar Fluids, Numerical Study, Stretching Cylinder.*

---

### 1. INTRODUCTION

The fluid flow about stretching surfaces is important due to its application in extrusion processes in plastic and metal industries. The flow due to stretching boundaries has been investigated for various situations such as permeable/ impermeable medium, magnetohydrodynamic (MHD) flows, heat transfer, stagnation point flow and non-Newtonian fluids flow. The phenomenon of boundary layer flow over the surfaces through which the fluid is either sucked or blown is useful to control the boundary layer and thermal effects for high energy flows. Several eminent researchers have investigated in detail the effects of suction/blowing on the flow due to stretching surfaces. It has been observed that the flow pattern is changed significantly because of the cooling produced by mass transfer and thus the heat transfer rate from the boundary surface is also affected.

Eringen [1] studied the one-dimensional flow problems for micropolar fluids. Guram and Smith [2] investigated the stagnation flows of micropolar fluids with strong and weak interaction. Anwar and Gurman [3] studied the flow of micropolar fluid confined between two infinite disks, one at rest and the other is rotating. Guram and Anwar [4] considered the steady, laminar and incompressible flow of a micropolar fluid due to a rotating disk with uniform suction and injection. Kamal and Hussain [5] analysed the flow of micropolar fluid inside an infinite channel. Kamal and Siddique [6] examined the time marching study of non steady, viscous incompressible micropolar fluids flow around a rotating and oscillating cylinder. Kamal, Ashraf and Syed [7] considered a two dimensional flow of a micropolar fluid driven by injection between two porous disks. Kamal and Siaft [8] investigated the stretching of a surface in a rotating micropolar fluid while Shafique and Rashid [9] obtained numerical solution of three dimensional micropolar flows due to a stretching flat surface. Sankara and Watson [10] investigated the steady micropolar flow past a stretching sheet. Crane [11] discussed a closed form exact solution of Navier-Stokes equations subject to two dimensional stretching of a flat surface. Brady and Acrivos [12] examined the exact similarity solutions of a flow inside a stretching channel and inside a stretching cylinder. Crane [13] found the boundary layer solution outside a stretching cylinder.

Watanabe and Oyama [14] studied maganatohydrodynamic boundary layer flow over a rotating disk. Dash and Tripathy [15] considered hydromagnetic fluid flow between two horizontal plates, both the plates being stretching sheets. Datta et al. [16] studied the effect of non-uniform slot injection/suction on a forced flow over a slender cylinder. Ishak et al. [17] analyzed the effects of uniform suction /blowing on flow and heat transfer for Newtonian fluid due to a stretching cylinder.

The fluid flow problem of Ishak et al. [17] is investigated for micropolar fluids. The similarity transformations have been used to reduce the governing differential equations to a system of ordinary differential equations. This system is solved numerically by using SOR method with Simpson (1/3) Rule. The solutions have been compared on different grid sizes. The comparison with the results for Newtonian fluids has also been shown. The numerical results have been discussed in graphical form.

**2. MATHEMATICAL ANALYSIS**

Eringen [1] offered the theory of micropolar fluids, the field equations of motion for micropolar fluids are given by:

$$\frac{\partial \rho}{\partial t} + \nabla \cdot (\rho \underline{V}) = 0 \quad , \tag{1}$$

$$(\lambda + 2\mu + \kappa) \nabla (\nabla \cdot \underline{V}) - (\mu + \kappa) \nabla \times (\nabla \times \underline{V}) + \kappa (\nabla \times \underline{\omega}) - \nabla \pi + \rho \underline{f} = \rho \left( \frac{\partial}{\partial t} + \underline{V} \cdot \nabla \right) \underline{V}, \tag{2}$$

$$(\alpha + \beta + \gamma) \nabla (\nabla \cdot \underline{\omega}) - \gamma (\nabla \times \nabla \times \underline{\omega}) + \kappa (\nabla \times \underline{V}) - 2\kappa \underline{\omega} + \rho \underline{l} = \rho j \left( \frac{\partial}{\partial t} + \underline{V} \cdot \nabla \right) \underline{\omega}, \tag{3}$$

with energy Equation

$$\rho C_p \left( \frac{\partial T}{\partial t} + (\underline{V} \cdot \nabla) T \right) = K \nabla^2 T + \Phi, \tag{4}$$

where  $\rho$  is the density,  $\underline{V}$  the velocity vector,  $\underline{\omega}$  the micro-rotation or spin,  $\pi$  the pressure,  $\underline{f}$  and  $\underline{l}$  the body force and the body couple per unit mass respectively,  $j$  the micro-inertia,  $\alpha, \beta, \gamma, \mu, \lambda$  and  $\kappa$  are material constants. The dissipation function is  $\Phi$  while  $T, C_p$  and  $K$  are fluid temperature, specific heat and heat conductivity respectively.

The equations of motion for micropolar fluids have been considered for this problem with the following assumptions:

- (i) The fluid flow is assumed to be steady, laminar and incompressible.
- (ii) The body force, the body couples and the viscous dissipation are neglected.
- (iii) The fluid flow is caused by a stretching tube of radius  $a$  in the axial direction in a fluid at rest where z-axis is taken along the axis of the tube and the r-axis is taken in the radial direction.
- (iv)  $T_w$  represents the constant temperature of the surface of the tube and  $T_\infty$  denotes the temperature of ambient fluid where  $T_w > T_\infty$ .
- (v) The velocity and microrotation vectors may be taken in the form  $\underline{V} = (u(r, z), 0, w(r, z))$  and  $\underline{\omega} = (0, \omega_2(r, z), 0)$ .

Under these assumptions, the set of equations (1) to (4) in cylindrical coordinates system become:

$$\frac{\partial u}{\partial r} + \frac{u}{r} + \frac{\partial w}{\partial z} = 0, \tag{5}$$

$$(\mu + \kappa) \left( \frac{\partial^2 u}{\partial r^2} + \frac{1}{r} \frac{\partial u}{\partial r} + \frac{\partial^2 u}{\partial z^2} - \frac{u}{r^2} \right) - \kappa \left( \frac{\partial \omega_2}{\partial z} \right) - \frac{\partial \pi}{\partial r} = \rho \left( u \frac{\partial u}{\partial r} + w \frac{\partial u}{\partial z} \right), \tag{6}$$

$$(\mu + \kappa) \left( \frac{\partial^2 w}{\partial r^2} + \frac{1}{r} \frac{\partial w}{\partial r} + \frac{\partial^2 w}{\partial z^2} \right) + \kappa \left( \frac{\omega_2}{r} + \frac{\partial \omega_2}{\partial r} \right) - \frac{\partial \pi}{\partial z} = \rho \left( u \frac{\partial w}{\partial r} + w \frac{\partial w}{\partial z} \right), \quad (7)$$

$$\begin{aligned} \kappa \left( \frac{\partial u}{\partial z} - \frac{\partial w}{\partial r} \right) - 2\kappa\omega_2 - \gamma \left( \frac{\omega_2}{r^2} - \frac{\partial^2 \omega_2}{\partial r^2} - \frac{1}{r} \frac{\partial \omega_2}{\partial r} - \frac{\partial^2 \omega_2}{\partial z^2} \right) \\ = \rho j \left( u \frac{\partial \omega_2}{\partial r} + w \frac{\partial \omega_2}{\partial z} + \frac{u\omega_2}{r} \right), \end{aligned} \quad (8)$$

$$\rho C_p \left( u \frac{\partial T}{\partial r} + w \frac{\partial T}{\partial z} \right) = K \left( \frac{1}{r} \frac{\partial T}{\partial r} + \frac{\partial^2 T}{\partial r^2} + \frac{\partial^2 T}{\partial z^2} \right). \quad (9)$$

Subject to the boundary conditions:

$$\begin{cases} u = u_w, & w = w_w, & T = T_w, & \text{at } r = a, \\ w \rightarrow 0, & T \rightarrow T_\infty, & & \text{as } r \rightarrow \infty, \end{cases} \quad (10)$$

where  $u_w = -ca\gamma$ ,  $w = 2cz$  with  $c$  being a positive constant of dimension [1/Time] and  $\gamma$  is a constant and it corresponds to mass injection for  $\gamma < 0$  and mass suction for  $\gamma > 0$ .

We now use the following similarity transformations to convert the equations of motion in dimensionless form:

$$\begin{cases} u = -caf(\eta) / \sqrt{\eta}, & w = 2cf'(\eta)z, \\ \omega_2 = -\frac{4c}{a^2} rzL(\eta) & \text{and } \theta = \frac{T - T_\infty}{T_w - T_\infty}, \end{cases} \quad (11)$$

where  $\eta = \left(\frac{r}{a}\right)^2$  is the dimensionless variable. The prime denotes the differentiation with respect to  $\eta$ .

If we substitute (11) in equation (5), then it may be verified that it is identically satisfied. We use (11) into equations (6) to (9) then after simplification we get:

$$\eta f''' + f'' - C_1(L + \eta L') = R(f'^2 - ff''), \quad (12)$$

$$4(2L' + \eta L'') - C_2(f'' - 2L) = C_3(\eta^{-1} fL + 2(fL' - f'L)), \quad (13)$$

$$\eta \theta'' + (1 + R \text{Pr } f)\theta' = 0, \quad (14)$$

where  $R = \frac{ca^2}{2\nu}$ ,  $\text{Pr} = \frac{\rho\nu C_p}{K}$  and  $\nu = \frac{\mu + \kappa}{\rho}$  are Reynolds number, Prandtl number and the coefficient of kinematics viscosity respectively.

It is interesting to note that the equations (12) and (13) reduce to the equation of motion for Newtonian fluids by vanishing micro rotation (or spin).

All  $C_1$ ,  $C_2$  and  $C_3$  are dimensionless constants given by

$$C_1 = \frac{\kappa}{\mu + \kappa}, C_2 = \frac{\kappa a^2}{\gamma} \text{ and } C_3 = \frac{a^2 \rho j c}{\gamma}. \text{ The dimensions of the parameters involved are as}$$

follows  $[\mu, \kappa] = MT^{-1}L^{-1}$ ,  $[\gamma] = MLT^{-1}$ ,  $[j] = L^2$ ,  $[\rho] = ML^{-3}$ ,  $[c] = T^{-1}$  and  $[a] = L$ .

In view of (11), the boundary conditions (10) take the form:

$$\begin{cases} f = \gamma, & f' = 1, & \theta = 1, & L = 0, & \text{at } \eta = 1, \\ f' \rightarrow 0, & \theta \rightarrow 0, & L \rightarrow 0, & & \text{as } \eta \rightarrow \infty. \end{cases} \quad (15)$$

The following equation can be determined from equation (4.2) as:

$$\frac{\partial \pi}{\partial r} = \frac{\rho c^2 a^4}{r^3} f^2 - \frac{2\rho c^2 a^2}{r} f' - \frac{4\mu cr}{a^2} f''.$$

The pressure  $\pi$  can be obtained from this equation by integration with respect to  $\eta$ .

For the purpose of numerical solution, it is convenient to reformulate the equations (12) to (14) by using:

$$\eta = e^x, \quad \eta \rightarrow 1 \text{ as } x \rightarrow 0. \tag{16}$$

Thus the equations (12) to (14) and boundary conditions (15) take the form:

$$f_{xxx} - 2f_{xx} + f_x - C_1 e^{2x}(L + L_x) = R(f_x^2 - ff_{xx} + ff_x), \tag{17}$$

$$4(L_{xx} + L_x) + C_2(e^{-x}(f_{xx} - f_x) - 2e^x L) = C_3(fL + 2(fL_x - f_x L)), \tag{18}$$

$$\theta_{xx} + R \text{Pr } f(x)\theta_x = 0, \tag{19}$$

and the boundary conditions are

$$\begin{cases} f = \gamma, \quad f_x = 1, \quad \theta = 1, \quad L = 0, & \text{at } x = 0, \\ e^{-x} f_x = 0, \quad \theta = 0, \quad L = 0, & \text{as } x \rightarrow \infty, \end{cases} \tag{20}$$

where the suffixes denote the differentiation with respect to  $x$ .

In order to solve the equations (17) and (18) numerically, we set:

$$P = f_x = \frac{df}{dx} \tag{21}$$

Then equations (17) and (18) become:

$$P_{xx} - 2P_x + P - C_1 e^{2x}(L + L_x) = R(P^2 - fP_x + fP), \tag{22}$$

$$\begin{cases} 4(L_{xx} + L_x) + C_2(e^{-x}(P_x - P) - 2e^x L) \\ = C_3(fL + 2(fL_x - PL)). \end{cases} \tag{23}$$

The boundary conditions (20) become:

$$\begin{cases} f = \gamma, \quad P = 1, \quad \theta = 1, \quad L = 0, & \text{at } x = 0, \\ e^{-x} P \rightarrow 0, \quad \theta \rightarrow 0, \quad L \rightarrow 0, & \text{as } x \rightarrow \infty. \end{cases} \tag{24}$$

Now, if we approximate the equations (22), (23) and (19) by central difference approximation at a typical point  $x = x_n$  of the interval  $[0, \infty)$ , we obtain

$$(2 - 2h + hRf_n)P_{n+1} + (2 + 2h - hRf_n)P_{n-1} - 2C_1 e^{2x} h^2 L_n - C_1 e^{2x} h(L_{n+1} - L_{n-1}) - (4 - 2h^2 + 2h^2 R(f_n + P_n))P_n = 0, \tag{25}$$

$$(8 + 4h - 2hC_3 f_n)L_{n+1} + (8 - 4h + 2hC_3 f_n)L_{n-1} + 2C_2 h^2 e^{-x} P_n - C_2 h e^{-x}(P_{n+1} - P_{n-1}) - (16 - 4C_2 h^2 e^x + 2C_3 h^2(f_n - 2P_n))L_n = 0, \tag{26}$$

$$(2 + hR \text{Pr } f_n)\theta_{n+1} + (2 - hR \text{Pr } f_n)\theta_{n-1} - 4\theta_n = 0, \tag{27}$$

where  $h$  denotes a grid size. For computational purposes, we shall replace the interval  $[0, \infty)$  by  $[0, \beta)$ , where  $\beta$  is sufficiently large.

We now solve numerically the first order ordinary differential equation (21) and the system of finite difference equations (25) to (27) at each interior grid point of the interval. The equation (21) is integrated by the Simpson's (1/3) rule with the formula of Adams-Moulton [18], where as the set of equations (25) to (27) are solved by using SOR iterative procedure [18] subject to the appropriate boundary conditions.

### 3. DISCUSSION ON NUMERICAL RESULTS

In this section, the results obtained by using the numerical computation for the problem reported in the previous section are presented in tabular as well as graphical form. In order to analyze velocity, temperature, microrotation, skin friction coefficient  $f''(1)$  and the Nusselt number  $-\theta'(1)$ , tables and curves have been drawn for representative values of the flow parameters namely  $R, \gamma$  and Pr. Three different sets of the material constants  $C_1, C_2$  and  $C_3$  given in the table below have been chosen arbitrarily and the results have been computed for each of the sets.

Case	$C_1$	$C_2$	$C_3$
I	0.1	0.2	0.3
II	0.05	0.1	0.2
III	0.02	0.15	0.25

For reliability of the present results, an extensive comparison of these results with the results for Newtonian fluids and the previously published results is given in the Table 1 to Table 3 for  $f''(1), f(\infty)$  and  $-\theta'(1)$  respectively. The results are in good agreement. It can be noticed from Table 1 that all the values of  $f''(1)$  are negative. It means that a dragging force on the fluid is exerted by the stretching tube. It can also be noted that absolute values of the skin friction coefficient  $f''(1)$  are larger for positive  $\gamma$  that stands for suction than negative  $\gamma$  that stands for injection. The asymptotic value  $f(\infty)$  decreases with increasing the values of  $R$  for every choice of  $\gamma$  as indicated in Table 2. The Table 3 shows that the heat transfer rate increases with increasing the values of  $\gamma$ . The Prandtl number Pr has no effect on the velocity components  $f$  and  $f'$ .

Graphically the results have been reported for a representative set of all the parameters of interest in the form of velocity and temperature distributions. Figure 1 to Figure 3 illustrate the effect of  $R$  on  $f$  for the values of  $\gamma = -0.5, 0$  and  $0.5$  respectively. It can be observed that the curves of  $f$  fall by increasing  $R$  for all selected values of  $\gamma$ . The behavior of  $f'(\eta)$  under the effect of  $R$  is shown in Figure 4 to Figure 6 for  $\gamma = -0.5, 0$  and  $0.5$  respectively. It is noticed that the velocity gradient at surface increases with increasing the values of  $R$ . Figure 7 illustrates the effect of  $\gamma$  upon the velocity function  $f'(\eta)$  for a fixed value of  $R=10$ . The velocity distributions in this figure indicate an increase in the velocity gradient at the surface with increase in the values of  $\gamma$ . This effect causes the increase in the wall shear stress and hence injection decreases the skin friction and suction increases it. This important finding may be applied to reduce the skin friction through injection. We note that the velocity profiles disappear for larger values of  $\eta$ .

Figure 8 and Figure 9 are drawn to observe the effect of Pr and  $\gamma$  upon temperature function  $\theta(\eta)$  for a fixed value of  $R=10$ . The curves have been presented in these figures for the values of Pr= 0.7(air) and 7.0(water) respectively when  $\gamma = -0.5, 0$  and  $0.5$ . In both the figures  $\theta(\eta)$  decreases with increase in the values of  $\gamma$  and then becomes zero at a large  $\eta$  in both the cases. It is noticed that the increasing values of  $\gamma$  decrease the thermal boundary layer for fixed value of Pr. This situation causes the increase in wall temperature gradient and thus the surface heat transfer rate is increased. So, the increasing values of  $\gamma$  increase the Nusselt number. Figure 10 and Figure 11 demonstrate the effect of  $\gamma$  on  $\theta(\eta)$  for large values of Pr and different values of  $R$ . It is observed that the temperature gradient at the surface becomes zero for strong injection. Hence, the heat transfer rate at the surface can be reduced by injection.

**Table 1:** The comparison of Micropolar fluids and Newtonian fluids for  $f''(1)$

$\gamma$	$R$	Micropolar fluids			Newtonian fluids	
		I	II	III	Present	Previous
<b>0.0</b>	0.1	-0.5443344	-0.4959164	-0.4974709	----	----
	0.5	-0.8940945	-0.8865318	-0.8864365	----	----
	1.0	-1.1846790	-1.1811456	-1.1810026	----	----
	2.0	-1.5997895	-1.5959939	-1.5958842	-1.595297	-1.5941
	5.0	-2.419663	-2.410713	-2.410623	-2.410499	-2.4175
	10.0	-3.343893	-3.318196	-3.318130	-3.318044	-3.3445
	15.0	-4.049064	-4.007159	-4.007102	----	----
	20.0	-4.645396	-4.582964	-4.583002	----	----
<b>-0.5</b>	0.1	-0.7039795	-0.4726658	-0.4748879	----	----
	0.5	-0.7866631	-0.7753430	-0.7752953	----	----
	1.0	-0.9702454	-0.9656963	-0.9655247	----	----
	2.0	-1.1857996	-1.1847553	-1.1846361	-1.184350	-1.1810
	5.0	-1.4831551	-1.4854964	-1.4854201	-1.485243	-1.4811
	10.0	-1.6790875	-1.6823539	-1.6823014	-1.682201	-1.6776
	15.0	-1.7694720	-1.7728433	-1.7728003	----	----
	20.0	-1.8207320	-1.8244752	-1.8244847	----	----
<b>0.5</b>	0.1	-0.5624542	-0.5193005	-0.5212460	----	----
	0.5	-1.0217437	-1.0115728	-1.0121593	----	----
	1.0	-1.0217437	-1.4420661	-1.4418277	----	----
	2.0	-2.147914	-2.142297	-2.142278	-2.141963	-2.1468
	5.0	-3.928305	-3.882791	-3.882786	-3.882652	-3.9308
	10.0	-6.592847	-6.435619	-6.435676	-6.435548	-6.6222
	15.0	-9.141375	-8.815743	-8.816062	----	----
	20.0	-11.649300	-11.090161	-11.090691	----	----

**Table 2:** The comparison of Micropolar fluids and Newtonian fluids for  $f'(\infty)$

$\gamma$	$R$	Micropolar fluids			Newtonian fluids	
		I	II	III	Present	Previous
<b>0.0</b>	0.1	5.03047	5.08722	5.17849	----	----
	0.5	2.58751	2.49823	2.51841	----	----
	1.0	1.72587	1.66509	1.67149	----	----
	2.0	1.13568	1.07165	1.07255	1.105823	1.0983
	5.0	0.59715	0.59275	0.59249	0.592566	0.5933
	10.0	0.38662	0.38595	0.38579	0.385362	0.3857
	15.0	0.30481	0.30354	0.30342	----	----
	20.0	0.25704	0.25719	0.25707	----	----
<b>-0.5</b>	0.1	3.47312	4.77174	4.86822	----	----
	0.5	2.44332	2.32914	2.35554	----	----
	1.0	1.62389	1.53774	1.54847	----	----
	2.0	1.03743	0.96814	0.97131	1.053649	1.0277
	5.0	0.52012	0.49748	0.49782	0.508461	0.5027
	10.0	0.30123	0.29274	0.29222	0.293924	0.2999
	15.0	0.21363	0.21300	0.21251	----	----
	20.0	0.16847	0.16869	0.16890	----	----
<b>0.5</b>	0.1	5.35898	5.40657	5.49090	----	----
	0.5	2.76231	2.68177	2.69876	----	----
	1.0	1.87652	1.82598	1.83089	----	----
	2.0	1.27285	1.24559	1.24662	1.252686	1.2524
	5.0	0.83030	0.82920	0.82931	0.828878	0.8291
	10.0	0.67528	0.67568	0.67568	0.675645	0.6757
	15.0	0.62075	0.62091	0.62090	----	----
	20.0	0.59200	0.59241	0.59241	----	----

**Table 3:** The comparison of Micropolar fluids and Newtonian fluids for  $-\theta'(1)$

$\gamma$	Pr	Micropolar fluids			Newtonian fluids	
		I	II	III	Present	Previous
<b>0</b>	0.1	1.035165	1.070427	1.058554	1.050543	----
	0.7	1.696729	1.713347	1.713609	1.702547	1.5683
	2.0	3.028202	3.026080	3.027701	3.026962	3.0360
	7.0	6.155849	6.156290	6.155157	6.155753	6.1592
	10.0	7.462382	7.462192	7.461810	7.462454	7.4668
	15.0	9.258533	9.258176	9.257985	9.258509	----
<b>-0.5</b>	0.1	0.925755	0.917530	0.942230	0.873923	----
	0.7	0.427651	0.423049	0.436163	0.406289	0.2573
	2.0	0.067350	0.066924	0.067877	0.067486	0.0600
	7.0	0.000070	0.000071	0.000143	0.000476	0.0000
	10.0	0.000000	0.000000	0.000000	0.000000	0.0000
	15.0	0.000047	0.000047	0.000000	0.000000	----
<b>0.5</b>	0.1	1.544690	1.569890	1.557302	1.546597	----
	0.7	4.276252	4.299116	4.282403	4.276681	4.1961
	2.0	11.01250	11.01169	11.01224	11.012555	11.1517
	7.0	33.66551	35.07629	35.07643	35.076481	36.6120
	10.0	48.66214	48.66192	48.66207	48.662162	51.7048
	15.0	70.20512	70.20503	70.20512	70.205160	----

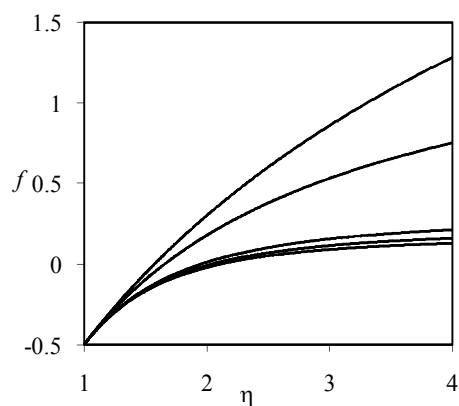


**Figure 1:** Graph of  $f$  for the values of  $\gamma = -0.5$  and  $R = 0.1, 2, 5, 10$  and  $20$  from top to bottom.

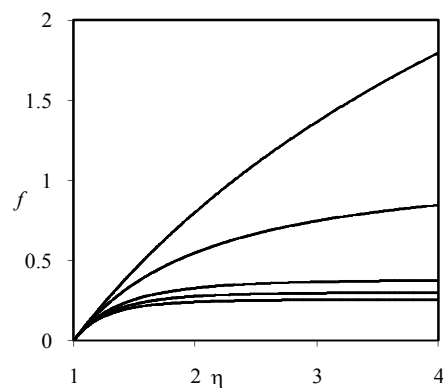


**Figure 2:** Graph of  $f$  for the values of  $\gamma = 0$ ,  $R = 0.1, 2, 5, 10$  and  $20$  from top to bottom.

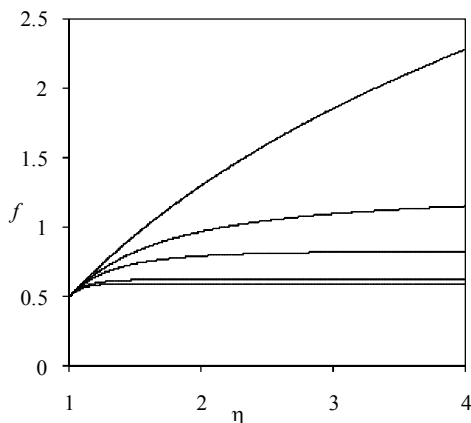


**Figure 3:** Graph of  $f$  for the values of  $\gamma = 0.5$ ,  $R = 0.1, 2, 5, 10$  and  $20$  from top to bottom.

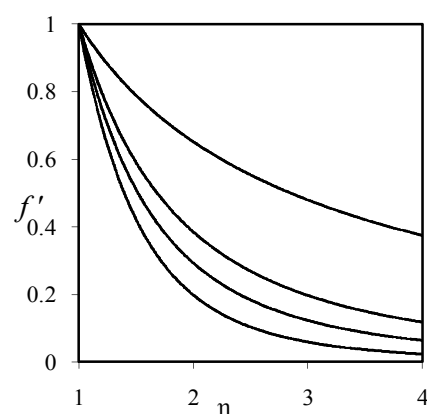


**Figure 4:** Graph of  $f'$  for the values of  $\gamma = -0.5$ ,  $R = 0.1, 2, 5$  and  $20$  from top to bottom.

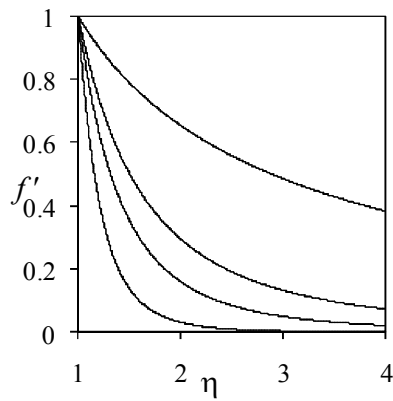


**Figure 5:** Graph of  $f'$  for the values of  $\gamma = 0$ ,  $R = 0.1, 2, 5$  and  $20$  from top to bottom.

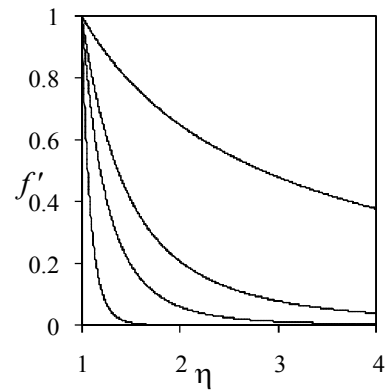


**Figure 6:** Graph of  $f'$  for the values of  $\gamma = 0.5$ ,  $R = 0.1, 2, 5$  and  $20$  from top to bottom.

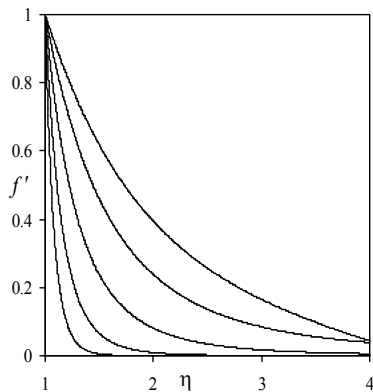


**Figure 7:** Graph of  $f'$  for the values of  $R = 10$ ,  $\gamma = -1.2, -0.5, 0, 0.5$  and  $1.2$  from top to bottom.

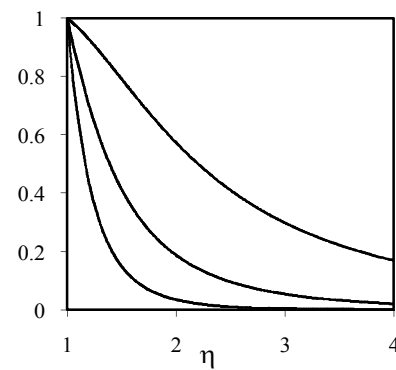


**Figure 8:** Graph of  $\theta(\eta)$  for the values  $Pr = 0.7$ ,  $R = 10$ ,  $\gamma = -0.5, 0, 0.5$  from top to bottom.

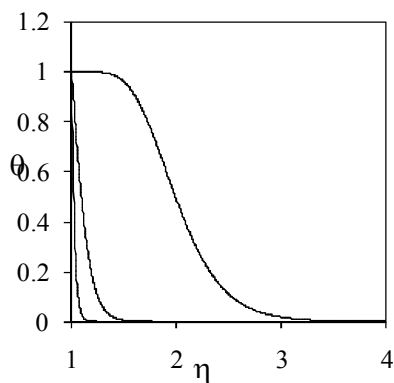


**Figure 9:** Graph of  $\theta(\eta)$  for the values  $Pr = 7, R = 10$ ,  $\gamma = -0.5, 0, 0.5$  from top to bottom.

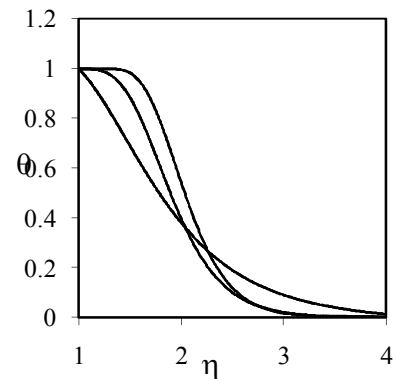


**Figure 10:** Graph of  $\theta(\eta)$  for  $Pr = 7, \gamma = -0.5$  and  $R = 1, 6, 12$  from bottom.

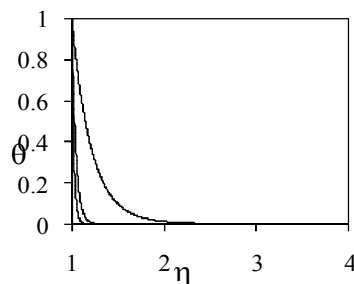


**Figure 11:** Graph of  $\theta(\eta)$  for the values  $Pr = 7, \gamma = 0.5$  and  $R = 1, 6$  and  $12$  from top to bottom.



## REFERENCES

- [1] Eringen, A.C. (1966). Theory of Micropolar Fluids. J. Math. Mech. 16, 1-18.
- [2] Guram, G. S. and Smith, A. C. (1980), Comp. and Math. with Appls.,6, 213-233
- [3] Anwar, M. and Guram, G.S. (1980), Micropolar fluid flow between a rotating and a stationary disc, Comp. and maths with appls., 6, 235-245.
- [4] Guram, G. S. and Anwar, M. (1981), ZAMM, 61, 589-595.
- [5] Kamal, M.A.and Sifat, H. (1994), Steady flow of a micropolar fluid in a channel with an accelerating surface velocity, Journal of Natural Sciences and Mathematics, 34(1), 23-40.
- [6] Kamal, M.A. and Siddiqui, A. Z. A. (2004), Micropolar fluid flow due to rotating and oscillating circular cylinder: 6th order numerical study, ZAAM, 82(2), 96.
- [7] Kamal, M. A., Ashraf, M. and Syed, K. S. (2006), Applied Math. and Computation,179, 1-10.
- [8] Kamal, M.A. and Sifat, H. (1994), Stretching of a surface in a rotating micropolar fluid, Int. J. of Sci. and Tech., Spring Hall, 30-36.
- [9] Shafique, M. and Rashid, A. (2006), Int. J. of Math. analysis, 1(2),173-187.
- [10] Sankara, K. K. and Watson, L. T. (1985), ZAMP, 36.
- [11] Crane, I.J. (1970), Zeit. Angew. Math. Phys., 21, pp645.
- [12] Bardy, J.F. and Acrivos, A. (1981), J. Fluid Mech., 112, pp127.
- [13] Crane, I.J. (1975), Zeit. Angew. Math. Phys., 26, pp619.
- [14] Watanabe, T. and Oyama, T. (1992), ZAAM, 71(12), 522-524.
- [15] Dash, G. C. and Tripathy, P. C. (1993), Modelling, Measurement and control, B, ASME Press, 51(2) , 51-64.
- [16] Datta, P., Anilkumar, D., Roy, S. and Mahanti, N.C. (2006), Effect of non- uniform slot injection/ suction on a forced flow over a slender cylinder, Int. J. Heat Mass Transfer , 49, 2366- 2371.
- [17] Ishak, A., Nazar, R. and Pop, I. (2008), Uniform suction / blowing effect on flow and heat transfer due to a stretching cylinder. Applied Mathematical Modelling, 32, 2059 – 2066
- [18] Gerald, C. F. (1989), Applied Numerical Analysis, Addison-Wesley Pub. NY.

## AUTHORS' BIOGRAPHY



**Dr. Mohammad Shafique:** He has been worked as a Assistant Professor in the Department of Mathematics Gomal University Dera Ismail Khan Pakistan for 22 years. He has obtained PhD from the above institution in 2012 and also has M.S. from McMaster University Canada in 1989. He has published six papers in 2013 as a principal and co-author. His field of interest in research is to find numerical solution of flows problems in micropolar fluids.



**Prof. Dr. Muhammad Anwar Kamal:** He is a retired professor in Applied Mathematics from BZ University, Pakistan. He has obtained PhD from Canada 1980. Now he is working as a professor of Mathematics, Al-Kharj University, Saudi Arabia. He has worked at ZB university in different capacities like DEAN and Director CASPAM. He has nearly 5 PhDs and plenty number of M.Phils to his credit. His papers more than 40 were published in various esteemed reputable International Journals. He is a Member of Various Professional Bodies. His field of interest in research and teaching in applied mathematics.